

Theoretical exploration of 2,2-bipyridines as electro-active
compounds in flow batteries

Supplementary Information

Mariano Sánchez-Castellanos^a, Martha M. Flores-Leonar^{ac}, Zaahel Mata-Pinzón^a,
Humberto G. Laguna^b, Karl García-Ruiz^a, Sergio S. Rozenel^a, Víctor M.
Ugalde-Saldívar^a, Rafael Moreno-Esparza^a, Joep J. H. Pijpers^{*d}, and Carlos
Amador-Bedolla^{*a}

^aFacultad de Química, Universidad Nacional Autónoma de México (UNAM), Av.
Universidad 3000, 04510, Coyoacán, CDMX, México. E-mail: carlos.amador@unam.mx

^bDepartamento de Química, Universidad Autónoma Metropolitana, Av. San Rafael
Atlixco 186, Col. Vicentina, 09340, Iztapalapa, CDMX, México

^cDepartment of Chemistry, University of Toronto, 27 King's College Circle, Toronto,
Ontario, Canada M5S 1A1.

^dInstituto Nacional de Electricidad y Energías Limpias (INEEL), Reforma 113, 62490,
Cuernavaca, Morelos, México. E-mail: jpijpers@ineel.mx

June 4, 2019

S1 Tables

Table S1: 3,3'-disubstituted-2,2'-bipyridines.

#	R	R'	E^0	pK_a
B3301	CH ₃	CH ₃	-0.99	3.12
B3302	OH	OH	-0.85	4.47
B3303	OCH ₃	OCH ₃	-0.91	3.33
B3304	CO ₂ H	CO ₂ H	-0.54	-0.73
B3305	CO ₂ CH ₃	CO ₂ CH ₃	-0.67	2.00
B3306	CO ₂ H	CO ₂ CH ₃	-0.62	-0.87

Table S2: 4,4'-disubstituted-2,2'-bipyridines.

#	R	R'	E^0	pK_a
B4401	CH ₃	CH ₃	-0.91	5.03
B4402	C ₉ H ₁₉	C ₉ H ₁₉	-1.02	3.93
B4403	(CH ₂) ₁₀ CH ₃	(CH ₂) ₁₀ CH ₃	-0.90	1.16
B4404	(CH ₂) ₁₁ CH ₃	(CH ₂) ₁₁ CH ₃	-0.89	4.94
B4405	(CH ₂) ₁₂ CH ₃	(CH ₂) ₁₂ CH ₃	-0.87	-0.94
B4406	(CH ₂) ₁₄ CH ₃	(CH ₂) ₁₄ CH ₃	-0.89	4.18
B4407	(CH ₂) ₁₈ CH ₃	(CH ₂) ₁₈ CH ₃	-0.91	7.13
B4408	CH ₃	CH ₂ CH ₂ OCH ₃	-0.90	4.28
B4409	CH ₃	CH=CH ₂	-0.88	4.02
B4410	CH=CH ₂	CH=CH ₂	-0.71	3.02
B4411	C≡CH	H	-0.77	4.22
B4412	C≡CH	C≡CH	-0.60	3.62
B4413	CH ₂ CH ₂ Ph	CH ₂ CH ₂ Ph	-0.90	4.75
B4414	PhCH ₃	PhCH ₃	-0.81	3.88
B4415	PhOH	PhOH	-0.81	3.94
B4416	PhOMe	PhOMe	-0.81	3.95
B4417	PhCl	PhCl	-0.72	3.15
B4418	Br	H	-0.72	2.31
B4419	Br	Br	-0.62	2.14
B4420	CH ₃	CH ₂ Br	-0.64	3.40
B4421	CH ₃	CH ₂ CH ₂ Br	-0.87	3.99
B4422	CH ₃	(CH ₂) ₃ Br	-0.91	4.63
B4423	CH ₃	(CH ₂) ₄ Br	-0.91	3.97
B4424	CH ₃	(CH ₂) ₅ Br	-0.91	4.47
B4425	CH ₃	(CH ₂) ₆ Br	-0.93	4.90
B4426	CH ₃	(CH ₂) ₇ Br	-0.89	3.98
B4427	PhCH ₂ Br	PhCH ₂ Br	-0.73	3.32
B4428	CH ₂ Br	CH ₂ Br	-0.62	2.49
B4429	C ₄ H ₈ Br	C ₄ H ₈ Br	-0.90	4.08
B4430	CH ₃	CH ₂ CH ₂ Cl	-0.89	4.27
B4431	CH ₂ Cl	CH ₂ Cl	-0.51	2.36
B4432	CH ₂ TMS	CH ₂ TMS	-0.89	4.02
B4433	CF ₃	CF ₃	-0.52	0.34
B4434	CH ₂ I	CH ₂ I	-0.30	3.90
B4435	CH ₃	(CH ₂) ₃ OH	-0.92	4.24
B4436	CH ₃	CH ₂ OH	-0.90	4.13
B4437	CH ₃	(CH ₂) ₄ OH	-0.89	4.66
B4438	CH ₂ OH	CH ₂ OH	-0.85	3.94
B4439	C ₄ H ₈ OH	C ₄ H ₈ OH	-0.92	4.57
B4440	OH	OH	-0.95	4.16

Table S3: 4,4'-disubstituted-2,2'-bipyridines (cont...).

#	R	R'	E^0	pK_a
B4441	OCH ₃	OCH ₃	-0.95	4.43
B4442	SCH ₃	SCH ₃	-0.85	3.19
B4443	SCH ₂ CH ₃	SCH ₂ CH ₃	-0.85	3.65
B4444	CH ₃	CHO	-0.70	3.58
B4445	CH ₃	(CH ₂) ₃ CHO	-0.90	4.35
B4446	CHO	CHO	-0.34	1.29
B4447	CH ₃	CN	-0.74	4.59
B4448	CH ₃	CH ₂ CH ₂ CN	-0.89	4.05
B4449	CN	CN	-0.36	0.97
B4450	CH ₃	CH ₂ CO ₂ H	-0.86	3.94
B4451	CH ₃	(CH ₂) ₃ CO ₂ H	-0.91	4.48
B4452	CO ₂ H	CO ₂ H	-0.40	1.02
B4453	COCl	COCl	-0.18	-0.46
B4454	CONHS	CONHS	-0.30	0.18
B4455	SO ₃ H	SO ₃ H	-0.31	-1.23
B4456	CH ₃	COCl	-0.55	2.54
B4457	COCl	CO ₂ CH ₂ CH ₃	-0.41	0.69
B4458	H	CO ₂ CH ₃	-0.74	3.21
B4459	CH ₃	CH ₂ CO ₂ CH ₃	-0.88	3.73
B4460	CO ₂ H	CO ₂ CH ₃	-0.45	1.27
B4461	CO ₂ CH ₃	CO ₂ CH ₃	-0.44	1.14
B4462	CH ₃	(CH ₂) ₄ NH ₂	-0.91	4.70
B4463	CH ₃	CH=NOH	-0.81	3.77
B4464	CH ₃	CH ₂ NH ₂	-0.91	4.57
B4465	CH ₂ CHOHPH	CH ₂ CHOHPH	-0.86	4.31

Table S4: 5,5'-disubstituted-2,2'-bipyridines.

#	R	R'	E^0	pK_a
B5501	CH ₃	H	-0.86	3.81
B5502	CH ₃	CH ₃	-0.90	4.03
B5503	C≡CH	H	-0.72	2.97
B5504	C≡CH	C≡CH	-0.60	1.45
B5505	C≡CSi(CH ₃) ₃	C≡CSi(CH ₃) ₃	-0.59	1.48
B5506	SiMe ₃	SiMe ₃	-0.77	3.93
B5507	Si ₂ Me ₅	Si ₂ Me ₅	-0.80	4.33
B5508	CH ₃	CH ₂ Br	-0.79	3.53
B5509	CH ₂ Br	H	-0.75	3.16
B5510	CH ₂ Br	CH ₂ Br	-0.65	2.03
B5511	CF ₃	CF ₃	-0.51	0.39
B5512	Br	H	-0.76	2.85
B5513	Br	Br	-0.62	0.41
B5514	Cl	H	-0.76	2.81
B5515	CH(CH ₃)OH	COCH ₃	-0.64	3.00
B5516	CH(CH ₃)OTBDMS	COCH ₃	-0.66	3.46
B5517	SH	SH	-0.76	2.18
B5518	CHO	H	-0.55	2.40
B5519	COCH ₃	COCH ₃	-0.43	1.23
B5520	CN	CN	-0.34	-0.99
B5521	H	SO ₃ H	-0.57	1.92
B5522	SO ₃ H	SO ₃ H	-0.29	-1.89
B5523	H	CO ₂ CH ₃	-0.65	2.78
B5524	CO ₂ Et	CO ₂ Et	-0.47	1.10
B5525	SCOCH ₃	H	-0.74	3.22
B5526	SCOCH ₃	SCOCH ₃	-0.63	1.20
B5527	SC(S)OEt	H	-0.70	2.74
B5528	SC(S)OEt	SC(S)OEt	-0.53	0.95
B5529	NH ₂	CO ₂ H	-0.75	3.29
B5530	NH ₂	CO ₂ Me	-0.79	3.56
B5531	NH ₂	CO ₂ Et	-0.79	3.37
B5532	NO ₂	CO ₂ Me	-0.27	0.57
B5533	NHCO ₂ Et	CO ₂ Et	-0.70	2.83
B5534	CON ₃	CO ₂ Et	-0.40	0.91
B5535	CONHNH ₂	CO ₂ Et	-0.51	1.26
B5536	CONHNH ₂	CONHNH ₂	-0.56	1.58
B5537	NH ₂	H	-0.96	4.76
B5538	NH ₃ Cl	NH ₃ Cl	0.26	1.85
B5539	CH ₂ NEt ₂	CH ₂ NEt ₂	-0.83	3.82
B5540	CH ₂ NMePh	CH ₂ NMePh	-0.82	3.58

Table S5: 5,5'-disubstituted-2,2'-bipyridines (cont...).

#	R	R'	E^0	pK_a
B5541	CH ₂ N(CH ₂ CH ₂ OH) ₂	CH ₂ N(CH ₂ CH ₂ OH) ₂	-0.82	3.42
B5542	N=CHPh	N=CHPh	-0.76	3.30
B5543	NO ₂	H	-0.32	1.73
B5544	NO ₂	NO ₂	-0.06	-2.16

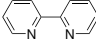
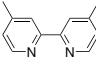
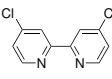
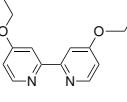
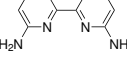
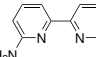
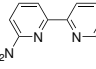
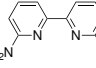
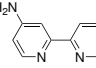
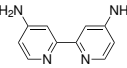
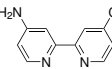
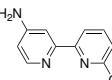
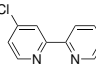
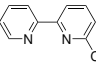
Table S6: 6,6'-disubstituted-2,2'-bipyridines.

#	R	R'	E^0	pK_a
B6601	CH ₃	CH ₃	-0.88	4.28
B6602	CH ₃	H	-0.87	4.59
B6603	CH ₂ CH ₃	H	-0.87	4.46
B6604	CH=CH ₂	CH=CH ₂	-0.73	3.71
B6605	C≡CH	C≡CH	-0.64	1.39
B6606	C≡CSi(CH ₃) ₃	C≡CSi(CH ₃) ₃	-0.63	1.06
B6607	CH ₂ Br	CH ₃	-0.84	4.17
B6608	CH ₂ Br	CH ₂ Br	-0.61	2.00
B6609	CH ₂ Cl	H	-0.80	3.20
B6610	CH ₂ Cl	CH ₂ Cl	-0.71	2.36
B6611	CF ₃	CF ₃	-0.54	-1.14
B6612	Br	CH ₃	-0.79	3.69
B6613	Cl	CH ₃	-0.80	3.71
B6614	Br	H	-0.74	2.81
B6615	Br	Br	-0.57	-2.01
B6616	Br	OC ₆ H ₁₃	-0.79	1.05
B6617	CH ₂ OTBS	H	-0.86	4.94
B6618	CH ₂ Cl	CH ₂ OH	-0.84	3.13
B6619	CH ₂ OH	CH ₂ OH	-0.83	3.41
B6620	CH ₂ OAc	CH ₂ OAc	-0.75	2.67
B6621	OCH ₃	OCH ₃	-0.86	1.76
B6622	OC ₆ H ₁₃	OC ₆ H ₁₃	-0.87	1.47
B6623	OMe	OMe	-0.86	1.76
B6624	OEt	OEt	-0.88	2.09
B6625	OPr	OPr	-0.86	2.11
B6626	OBu	OBu	-0.87	2.26
B6627	OHex	OHex	-0.87	1.47
B6628	manisyl	manisyl	-0.82	3.64
B6629	CH(OH)CH ₃	CH(OH)CH ₃	-0.85	3.68
B6630	CH(OAc)CH ₃	CH(OAc)CH ₃	-0.85	3.37
B6631	CHOCH ₃	CHOCH ₃	-0.85	4.01
B6632	SEt	H	-0.81	3.37
B6633	CHO	CHO	-0.38	0.59
B6634	COCH ₃	COCH ₃	-0.49	0.19
B6635	CO ₂ H	CO ₂ H	-0.45	-3.94
B6636	H	CO ₂ CH ₃	-0.76	2.82
B6637	CN	CN	-0.41	-2.28
B6638	CH ₂ NH ₂	CH ₂ NH ₂	-0.92	5.63
B6639	NH ₂	NH ₂	-1.02	5.60
B6640	NH ₂	NHC ₁₂ H ₂₅	-1.07	6.22
B6641	NHC ₁₂ H ₂₅	NHC ₁₂ H ₂₅	-1.04	5.42

S2 E and pK_a calibrations

Calculations for E and pK_a values were calibrated with a set of molecules whose experimental value was reported or measured experimentally. For the pK_a a set of 14 n,n-disubstituted-2,2-bipyridines (shown in Table S7) was calculated for the first protonation (reaction A in Figure 2) with the methodology described in the main article. The correlation between calculated and experimental values are shown in Figure S1 for PCM and SMD solvation models.

Table S7: Molecules used in the calibration of pK_a and their experimental values.

Number	Structure	$pK_a(\text{exp})$	Ref
1		4.30	[1]
2		5.42	[1]
3		2.80	[1]
4		5.70	[1]
5		6.72	[2, 3]
6		5.80	[3]
7		5.70	[3]
8		5.60	[3]
9		8.10	[3]
10		8.80	[3]
11		7.40	[3]
12		7.70	[3]
13		3.80	[3]
14		3.70	[3]

From the calibration we selected SMD solvation model as a better approach to estimate pK_a values, with correlations of 0.9667 and 0.9763 for pK_a values calculated with E_{elec} and G respectively. With this fitting we calibrate the calculated values ($pK_{a(\text{calc})}$) for the set of 156 n,n-disubstituted-2,2-bipyridines to get the best predicted values ($pK_{a(\text{pred})}$).

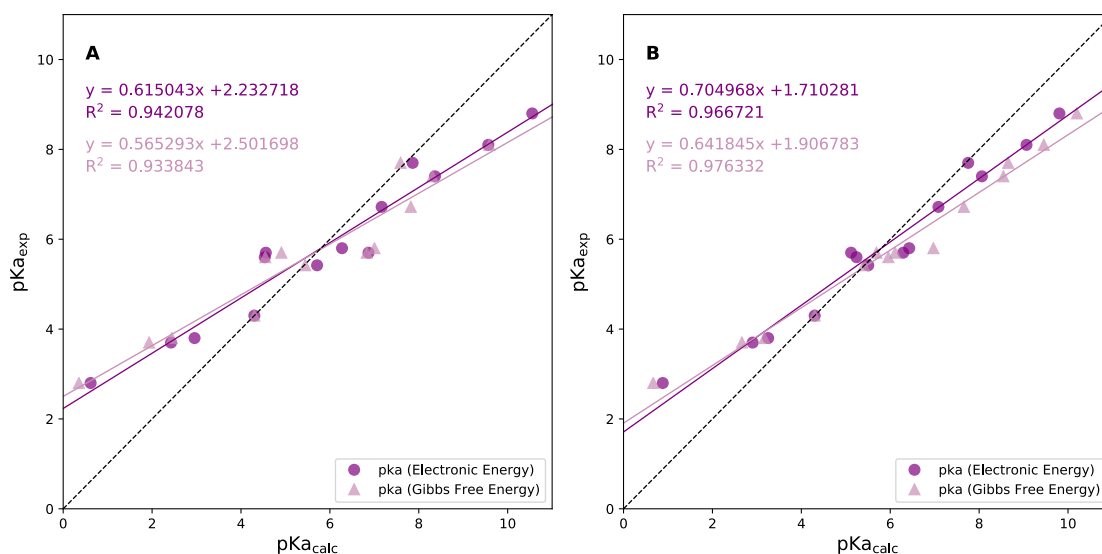
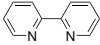
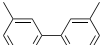

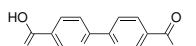
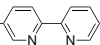


Figure S1: Correlation between calculated and experimental pK_a values for a set of 14 molecules. Calculations performed for the first protonation (reaction A), with A) PCM solvation model and B) SMD solvation model.

For the redox potentials we prepared a set of molecules whose E^0 values were measured experimentally under the conditions reported in the experimental methodology. First we calculate and calibrate the pK_a for the set of molecules. These pK_a 's were used to estimate the pH of measurement for the redox potentials. To ensure all molecules were protonated we consider a pH of measurement one unit below the predicted pK_a value. Results are shown in Table S8 and the respective correlation between the calculated and experimental redox potentials are shown in Figure S2.

Table S8: Molecules used in the calibration of redox potentials (E). $pK_{(a2)}^o$ and $pK_{(a1)}^r$ predicted values, experimental pH values and redox potentials (E) measured.

Number	Structure	pK_{a2}^o	pK_{a1}^r	pH_{exp}	E_{exp}
1		4.66	2.98	3.6	-0.826
2		5.38	3.63	4.3	-0.879
3		5.76	3.72	4.7	-0.942
4		1.69	-1.49	0.6	-0.385
5		5.26	3.49	4.2	-0.904

The calibration shows that the calculated redox potentials are in agreement with the experimental ones with a correlation greater than 0.99 for both solvation models and energies used in the calculations.

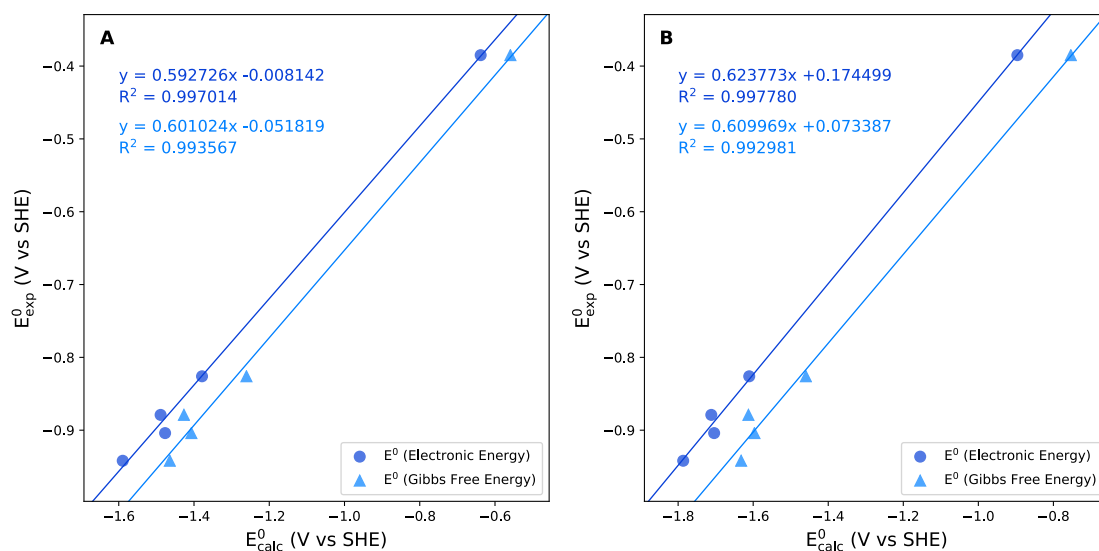


Figure S2: Correlation between calculated and experimental redox potentials for a set of five molecules. Calculations performed for reaction 3 with A) PCM solvation model and B) SMD solvation model.

Redox potentials for the 156 n,n'-disubstituted-2,2'-bipyridines were calculated and calibrated for all reactions present in the PCET scheme (Figure 2 in the main article). The distribution of the predicted values is observed in Figure S2 for the SMD solvation model. On the screening procedure molecules with deviated values considered as outliers were taken off the distribution. These deviated outliers values were analyzed and are associated to optimizations that lead to a bond breaking of the reduced species. This indicates possible decomposition reactions associated to the electron transfer in reactions 14, 14, 11 and 4 molecules for reactions 2, 4, 5 and 6 respectively. Some examples of these decomposition reactions are shown in Figure S3.

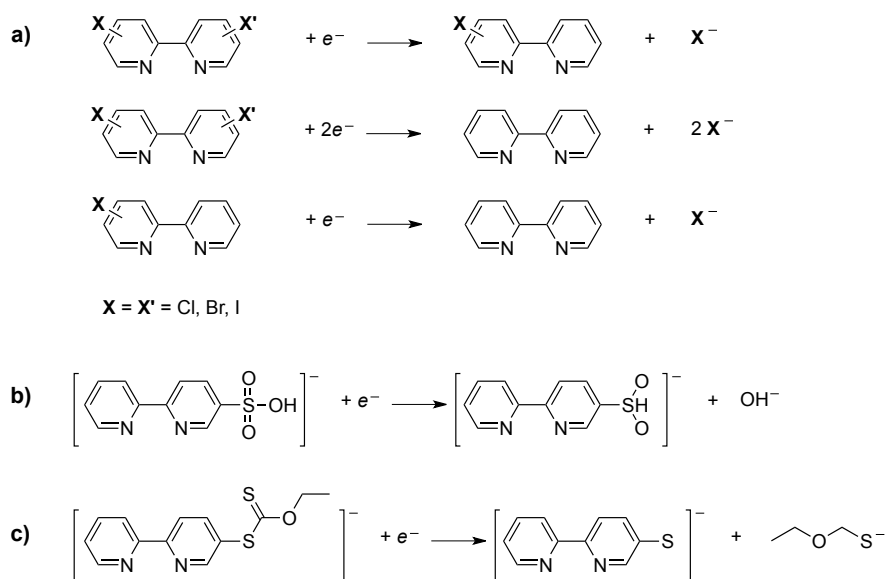


Figure S3: Decomposition reactions found in the screening of redox potentials. a) Halogen decomposition found for one and two electron transfers (reactions 1 and 1-2 respectively). b) Sulfonate decomposition and c) dithio decomposition found for the second electron transfer (reaction 2).

S3 Estimation of aqueous solubility

Xu's model use Equation S3 to describe the contribution to $\log S$ (the logarithm of the intrinsic solubility) of each atomic subunit that constitutes the molecule, namely

$$\log S = C_D + \sum_i a_i n_i + \sum_j b_j B_j$$

where a_i is the contribution of the i -eth subunit, b_j are correction factors, n_i and B_j are the corresponding occurrences for coefficients a_i and b_j , and C_D the solvent constant (for group types, contributions and correction factors see references [4, 5]).

Models based on Equation S3 can be easily extended incorporating different descriptors and correction factors (a comprehensive review can be found in reference [5]). In Xu's model Solvent Accessible Surface Area (SASA) descriptor is included, which considers the relative interactions between solute-solute, solute-water and water-water, and that more exposed atoms have bigger contributions than inner ones [6]. However, we use Xu's model without SASA descriptor [4] because our results show that no significant improvements are observed and yet we can gain computer time with a more simplified model.

Calibration consisted in comparing our results ($\log S$) against the experimental and theoretical values of Xu's [4] and Yalkowsky's [7] data sets in order to validate our methodology (see Figs. 4-7). In the case of Yalkowsky's set (18 molecules), theoretical predictions were calculated by Xu et al. and are labeled as $\log S_{YH}$, while experimental values are identified as $\log S_{YE}$; in the case of Xu's data (50 molecules), experimental values are labeled as $\log S_{HE}$ and theoretical values as $\log S_{HH}$.

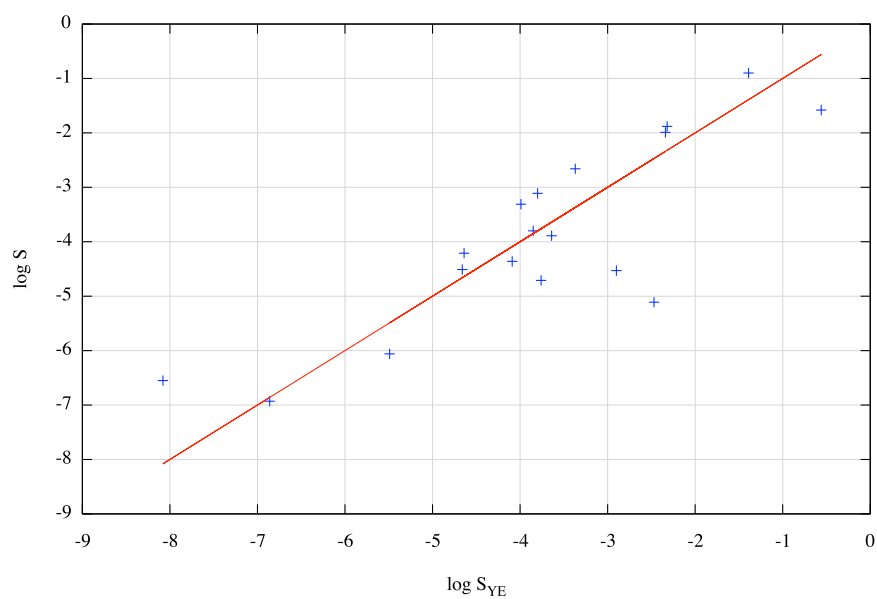


Figure S4: Calibration using Yalkowsky's experimental data set ($\log S_{YE}$). Correlation coefficient $r = 0.8446$ with $\log S = 0.7909 \log S_{YE} - 0.8966$.

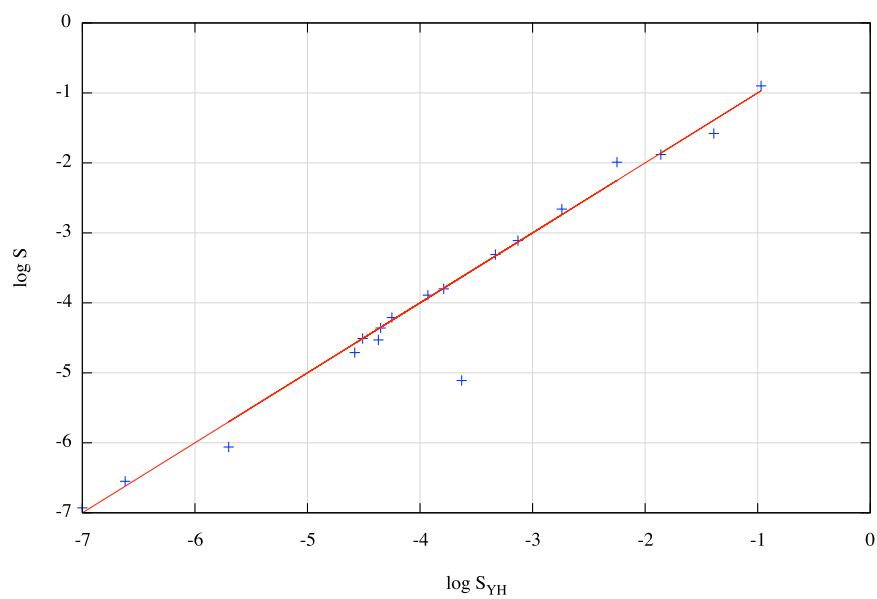


Figure S5: Calibration using Yalkowsky's theoretical data set ($\log S_{YH}$). Correlation coefficient $r = 0.9578$ with $\log S = 1.0090 \log S_{YH} - 0.0607$.

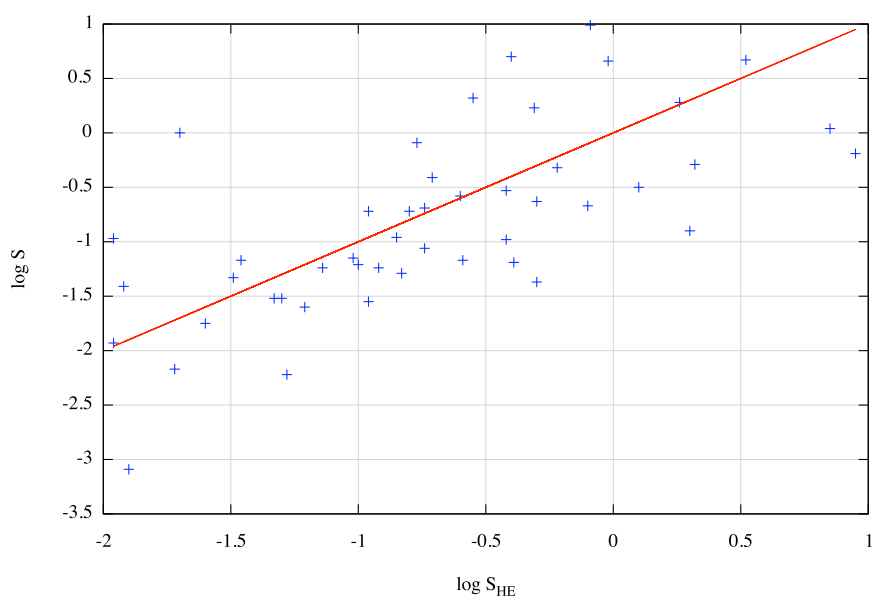


Figure S6: Calibration using Xu’s experimental data set ($\log S_{HE}$). Correlation coefficient $r = 0.6746$ with $\log S = 0.7739 \log S_{HE} - 0.2633$.

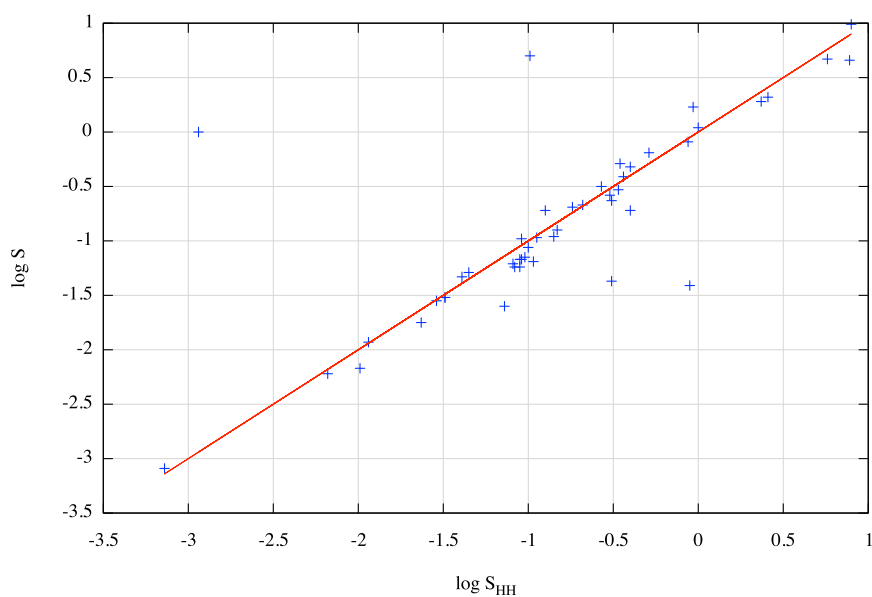


Figure S7: Calibration using Xu’s theoretical data set ($\log S_{HH}$). Correlation coefficient $r = 0.7712$ with $\log S = 0.7605 \log S_{HH} - 0.1838$.

Figures S5 and S7 show that our theoretical results do not differ significantly from the corresponding Xu’s and Yalkowsky’s sets, proving that our errors are similar to those of the theoretical framework proposed by Xu et al. Comparison between calculated $\log S$ and experimental data for both sets (Figs. S4 and S6), exhibit a sufficiently good correlation that allow us to validate our methodology.

It has been mentioned in the manuscript that oxidized species have bigger absolute values for ΔG_{solV} ,

however, for log S values and the general behaviour between both properties, not considerably differences can be observed. To prove the above, ΔG_{solv} and log S values between species HBpy^+ and HBpy were compared and results depicted in Figures S8 and S9.

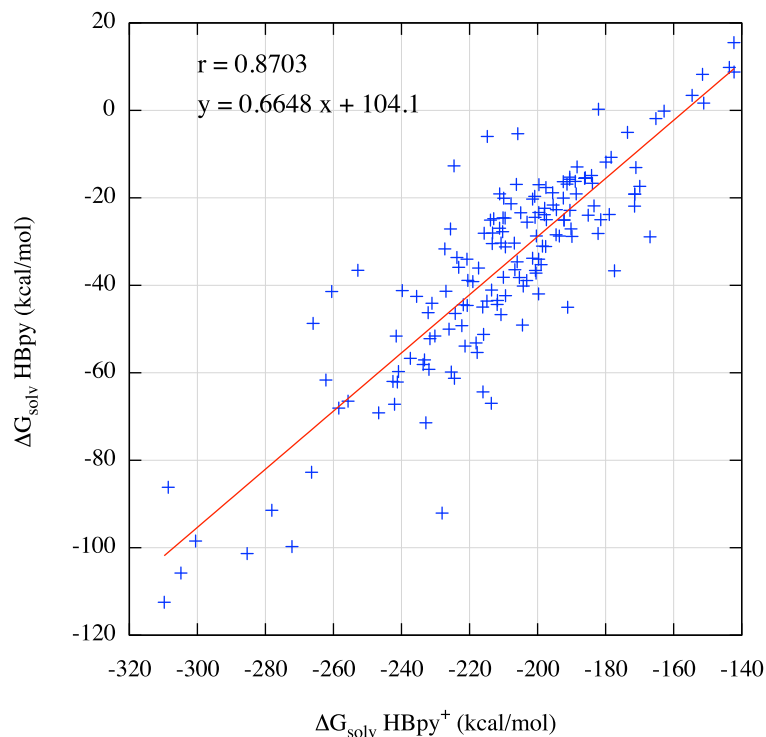


Figure S8: Comparison of ΔG_{solv} energies between species HBpy^+ and HBpy .

Figure S8 shows that ΔG_{solv} energies of both species are fair enough correlated, which can be explained because charged molecules, in general, need greater absolute values for ΔG_{solv} . Therefore, the shift towards these values for charged molecules is linear as it was supposed. In Figure 9 it is observed that in the case of log S this correlation is even stronger, and so solubility it is not considerably affected by the presence of charge molecules.

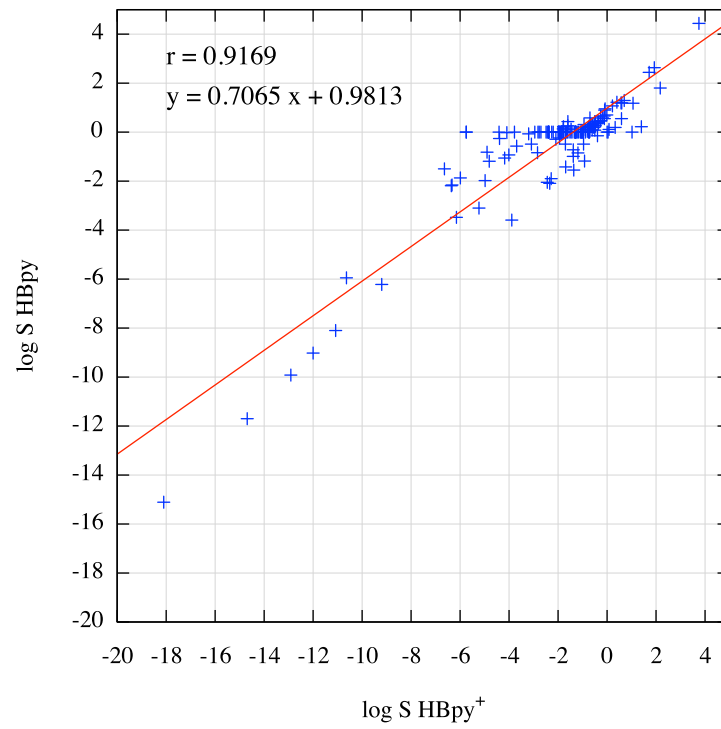


Figure S9: Comparison of $\log S$ values between species $HBpy^+$ and $HBpy$.

S4 Reduced 2,2'-bipyridines

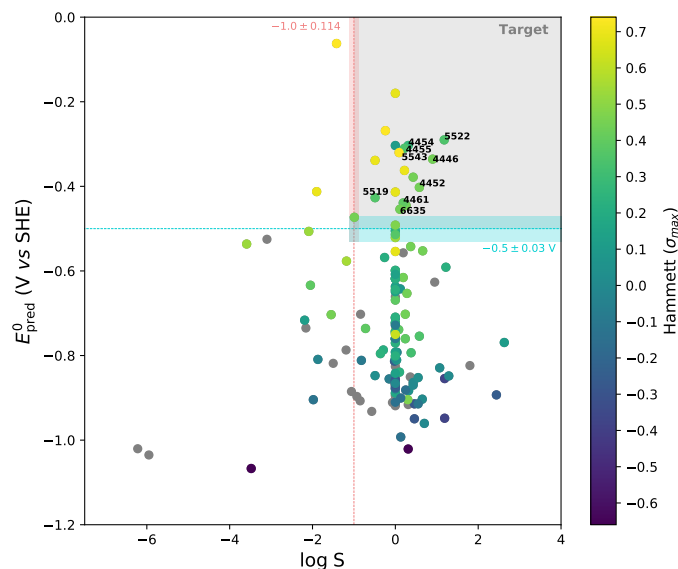


Figure S10: Standard reduction potential values of 2,2'-bipyridines as function of logarithmic solubility values ($\log S$) for HBPy calculated with ChemAxon software and their corresponding Hammett substituent factor.

References

- [1] W.A.E. McBryde. A critical review of equilibrium data for proton- and metal complexes of 1,10-phenanthroline, 2,2-bipyridyl and related compounds. In W.A.E. McBRYDE, editor, *A Critical Review of Equilibrium Data for Proton and Metal Complexes of 1,10-phenanthroline, 2,2'-Bipyridyl and Related Compounds*, pages 1 – 17. Pergamon, 1978.
- [2] Noriyuki Kishii, Koji Araki, and Shinsaku Shiraishi. The changes in conformation and complexability of 6,6-diamino-2,2-bipyridine by protonation. *Bulletin of the Chemical Society of Japan*, 57(8):2121–2126, 1984.
- [3] Koji Araki, Toshiki Mutai, Yasuhiro Shigemitsu, Masaki Yamada, Takayoshi Nakajima, Shigeyasu Kuroda, and Ichiro Shima. 6-amino-2,2-bipyridine as a new fluorescent organic compound. *J. Chem. Soc., Perkin Trans. 2*, pages 613–617, 1996.
- [4] T. J. Hou, K. Xia, W. Zhang, and X. J. Xu. Adme evaluation in drug discovery. 4. prediction of aqueous solubility based on atom contribution approach. *Journal of Chemical Information and Computer Sciences*, 44(1):266–275, 2004. PMID: 14741036.
- [5] Junmei Wang, George Krudy, Tingjun Hou, Wei Zhang, George Holland, and Xiaojie Xu. Development of reliable aqueous solubility models and their application in druglike analysis. *Journal of Chemical Information and Modeling*, 47(4):1395–1404, 2007. PMID: 17569522.

- [6] Tingjun Hou, Xuebin Qiao, Wei Zhang, and Xiaojie Xu. Empirical aqueous solvation models based on accessible surface areas with implicit electrostatics. *The Journal of Physical Chemistry B*, 106(43):11295–11304, 2002.
- [7] Yingqing Ran, Neera Jain, and Samuel H. Yalkowsky. Prediction of aqueous solubility of organic compounds by the general solubility equation (gse). *Journal of Chemical Information and Computer Sciences*, 41(5):1208–1217, 2001. PMID: 11604020.